RADARGRAMMETRY WITH CHANDRAYAAN-1 AND LRO MINI-RF IMAGES OF THE MOON: CONTROLLED MOSAICS AND DIGITAL TOPOGRAPHIC MODELS. R.L. Kirk[1], D. Cook[1], E. Howington-Kraus[1], J.M. Barrett[1], T.L. Becker[1], C.D. Neish[2], B.J. Thomson[2], D.B.J. Bussey[2] and the Mini-RF Science Team. [1]Astrogeology Science Center, U.S. Geological Survey, 2255 N. Gemini Dr., Flagstaff AZ 86001 (rkirk@usgs.gov), [2]The Johns Hopkins University Applied Physics Laboratory, Laurel, MD 20723.

Introduction: The Mini-RF investigation [1] consists of two synthetic aperture radar (SAR) imagers for lunar remote sensing: Mini-SAR (also known as "Forerunner"), which was flown on the ISRO Chandrayaan-1 orbiter in November 2008, and the Mini-RF technology demonstration, which was flown on the NASA Lunar Reconnaissance Orbiter (LRO) in June 2009. A primary objective for both instruments was to investigate the possible presence of water ice in permanently shadowed areas near the lunar poles [2]. Not only can these imagers "see in the dark" by providing their own illumination, they measure the full polarization characteristics of the reflected signal for circularly polarized transmitted radiation [3]. A strong return in the "unexpected" (i.e., not reversed as it would be if reflected from a smooth interface) sense of circular polarization can be indicative of radar-transparent materials such as ice (e.g., [4]). Mini-SAR obtained nearly complete image coverage of both lunar poles to 80° latitude with a resolution of 150 m and radar wavelength of 12.6 cm (S Band), as well as images of non-polar targets for comparison purposes. LRO Mini-RF is capable of imaging in both S-Band and X-band (3 cm) wavelengths and at 150 m and 30 m (zoom mode) resolutions. (The 3-cm wavelength is actually in the C-Band but is referred to as X-Band because early designs used a wavelength in this band.) Most of its observations to date have been obtained in S-Band zoom mode, and include both right- and left-looking coverage of much of the south polar zone in support of the LCROSS mission [5] as well as extensive non-polar coverage.

In this abstract we describe the software and techniques we are developing for radargrammetric analysis of the Mini-RF images. These tools will enable us to make controlled image mosaics with both image-to-image seam errors and absolute positional accuracy improved by at least an order of magnitude compared to uncontrolled products. They will also permit the derivation of digital topographic models (DTMs) from stereo pairs of radar images, from which orthoimages (images from which topographic parallax distortions have been removed), slope maps, and other products can be generated. A primary motivation for both types of processing is to coregister the radar images as closely as possible to one another and to other datasets [6], so that detailed analyses can be made. Comparison of multiple polarization measurements, correction of these results for locally varying incidence angles (i.e., slope effects), and improved topographic data for determining what areas are permanently shadowed are logical extensions of preliminary work such as [7] and should all lead to firmer conclusions about the presence of ice at the lunar poles. Precise georeferencing of the images will also be essential to using them in studies of the LCROSS impact point. Coregistration of Mini-RF images with a variety of spectrophotometric data should also shed light on interesting sunlit features, for example pyroclastic deposits [8].

We note in passing that Mini-RF, with intermediate resolution between those of the LROC narrow-angle and wide-angle cameras, is ideally suited for completing a uniform global topographic model of the Moon. Data from the LOLA laser altimeter have unprecedented meter-scale accuracy, but LOLA tracks will typically be separated by a kilometer or more at low latitudes [9]. These gaps could be filled by DTM data derived from zoom mode stereopairs and controlled to be consistent with LOLA by using the techniques described here.

Radargrammetry: Radargrammetry is the art and science of making geometric measurements based on radar images, and is precisely analogous to photogrammetry but takes account of the different principles by which a radar image is formed. The fundamental tool in both cases is a *sensor model*, which allows one to calculate the image coordinates (line and sample) of any point whose latitude, longitude, and elevation are specified, or the latitude and longitude of any image pixel provided the elevation is specified. The sensor model is needed to transform image pixels into their appropriate locations in map coordinates. It is also used to make controlled image mosaics that have improved accuracy by *bundle adjustment*, in which the spacecraft positions are adjusted to achieve the best least-squares agreement between the positions of features in overlapping images and between the images and pre-existing ground control. Finally, the sensor model is used to turn a dense set of feature correspondences between a pair of images, obtained either by automated image matching or interactively, into a DTM.

Our approach to radargrammetric processing of Mini-RF images follows that which we have applied to numerous optical sensors and to the Magellan and Cassini radar imagers [10–12]. In particular, we use the USGS in-house cartographic software system ISIS [13] to ingest and prepare the data, project images onto a known reference surface (sphere, ellipsoid, or DTM), and perform a variety of general image analysis and enhancement tasks. We use a commercial digital photogrammetric workstation running SOCET SET (® BAE Systems) software [14] for DTM production by automated matching and for interactive editing of DTMs using its stereo display capability. Using this commercial system with a given data set requires not only an appropriate sensor model, but also software to translate the images and supporting information from ISIS to SOCET SET formats.

A key difference between Mini-RF and the Magellan and Cassini SARs is that data from these earlier instruments were produced only in map-projected form. As a result, we used ISIS capabilities for transforming data from one projection to another to make uncontrolled mosaics but did not implement an ISIS sensor model for these missions. Instead, we created sensor models for SOCET SET that worked by first "undoing" the map projection to get back to the fundamental radar image coordinates of range and Doppler shift. These sensor models perform rather complex bookkeeping so they work with mosaics of multiple orbits (Magellan) or multiple radar beams (Cassini). They can be used to perform bundle adjustments and produce DTMs. In contrast, the Mini-RF data [15] are produced and archived both in "Level 2" map coordinates [16] and in "Level 1" coordinates that are similar but not identical to the raw camera geometry for a pushbroom scanning camera.

ISIS Software: Given the availability of Mini-RF data in Level 1 instrument coordinates, we have implemented a sensor model for the ISIS 3 system, based on the physical principals of SAR image formation. We have verified that map-projecting Level 1 images with this sensor model yields results consistent with the Level 2 products from the Mini-RF processing pipeline developed by Vexcel Corporation. This apparently redundant capability is valuable for several reasons. First, image projection in ISIS can potentially make use of improved spacecraft trajectory data in the form of SPICE kernels [17] and improved topographic models onto which to project the images as these become available. Second, we have also incorporated the Mini-RF sensor model into the ISIS bundle-adjustment program "jigsaw" so that images can be controlled to yield even higher accuracy. Finally, and most importantly, the ISIS software (unlike either SOCET SET or the Vexcel SAR processor) is freely

available and can be used by anyone to make controlled mosaics and other products from Mini-RF images. The system includes software needed to ingest both Level 1 and Level 2 data products archived in NASA Planetary Data System (PDS) format. All software elements are equally compatible with both Chandrayaan-1 and LRO images.

SOCET SET: We are currently implementing a Mini-RF sensor model for SOCET SET, as well as the software needed to translate images and spacecraft trajectory data (in SPICE SPK format) to SOCET formats. The sensor model operates on identical principles to that already developed for ISIS, and is substantially simpler than our past Magellan [9] and Cassini [10] models. Once the model is completed, all SOCET SET functions will be available for Chandrayaan-1 and LRO Mini-RF images in combination with one another or, if desired, with any other supported images. The bundle adjustment capability of SOCET SET will provide a useful check of the validity of results from ISIS "jigsaw" but the main application will be DTM production by a combination of automatic image matching and interactive editing. The commercial software and special display hardware it uses are relatively expensive, but several planetary investigators have SOCET workstations at their home institutions (see, e.g., [18]). The USGS has several such workstations used for mapping under the NASA Planetary Cartography program and various flight programs, and one that is operated as a guest facility at which outside researchers can make their own DTMs from publically available data [19].

Test Data and Prospects: By far the most extensive sets of overlapping SAR images are in the areas poleward of 80° north and south. Forerunner images covering >90% of these regions were obtained. LRO Mini-RF S-zoom mode images cover a smaller but still appreciable fraction of the south polar zone at higher resolution [5]. Both datasets provide a mixture of eastward and westward viewing and illumination direction; although the look direction (left or right of the ground track) is constant for each image strip, the compass directions of illumination on the ascending and descending sides of the orbit are opposite. The south polar zone, in particular, the 98 km diameter crater Cabeus in which the LCROSS spacecraft impacted, is therefore the highest priority for controlled mosaic and DTM production, results of which will be presented in our poster. Visual inspection indicates that image-to-image offsets of as much as several km are found in the image sets from both missions, despite the expectation of spacecraft positioning errors ≤500 m for Chandrayaan-1 and ≤100 meters for LRO. Our experience with Cassini data indicates that radargrammetric bundle adjustment can reduce these relative errors to on the order of the pixel size (roughly half the image resolution) even in the presence of substantial speckle noise in the images. Thus, precisions on the order of 100 m and 10 m or better should be achievable for Chandrayaan-1 and LRO zoom data, respectively. The accuracy of absolute positioning depends on the availability of suitable reference data to provide ground control and is probably on the order of 100 m for LOLA altimetric data in their initial state.

The properties of stereo DTMs depend on the resolution and viewing directions of the source imagery. The opposite-look LRO S-zoom images (Fig. 1) have high resolution and strong image convergence. Standard formulas of radargrammetry indicate that the expected vertical precision (EP) for these images is on the order of 10 m, if image matching is precise to half the resolution as we have found to be the case for Cassini radar [11]. Horizontal resolution of the DTM can be expected to be a few times the resolution, or on the order of 50-100 m. The differences in surface shading may, however, make matching of these oppositely illuminated images challenging. Same-side images from LRO and Chandrayaan-1, which have incidence angles of 47.6° and 33.5° respectively, could be used but the relatively weak geometry and worse resolution of the latter would lead to an EP of ~120 m and horizontal resolution of at least 500 m. We plan to experiment with DTM production from these image combinations in order to verify the precision and resolution that can be achieved in practice.

A total of 15 non-polar images were obtained by Chandrayaan-1, one of which has already been re-imaged by LRO. As described above, radar stereo imaging by LRO has tremendous potential for filling in the topographic map of the Moon's equatorial zone. DTM properties for these types of stereopairs would be similar to the LRO-Chandrayaan and LRO-LRO polar data sets discussed above.

Concluson: We have implemented a series of radargrammetric tools for processing Chandrayaan-1 and LRO Mini-RF radar images of the Moon. These tools will be used within the Mini-RF team to make high-precision controlled mosaics and digital topographic models. Through the open release of ISIS software and the USGS/NASA Planetary Photogrammetry Guest Facility, the same capabilities will soon be available to the entire planetary research community.

References: [1] Nozette, S. et al. (2009) *Space Sci. Rev*., in press. [2] Bussey, D.B.J. et al. (2003) *GRL, 30*, 7158. [3] Raney, R.K. (2007) *IEEE Trans Geosci. Remote Sens. 45*, 3397. [4] Harmon, J.K. et al. (2001) *Icarus, 149*, 1. [5] Neish, C.D. et al. (2010) *LPS XLI*, this conference. [6] Archinal, B.A. et al. (2010) *LPS XLI*, this conference. [7] Thomson, B.J. et al. (2010) *LPS XLI*, this conference. [8] Carter, L.M., et al. (2010) *LPS XLI*, this conference; Trang, D. et al. (2010) *LPS XLI*, this conference. [9] Smith, D.E. et al. (2009) *Space Sci. Rev*. doi:10.1017/s11214-009-9512-y. [10] Howington-Kraus, E. et al. (2002) *LPS XXXIII*, 1986. [11] Kirk, R.L. et al. (2010) *Icarus*, in revision. [12] Kirk, R.L. et al. (2008) *IAPRSSIS XXXVII*(4), 973. [13] Anderson, J.A. et al. (2004) *LPS XXXV*, 2039. [14] Miller, S.B., and A.S. Walker (1993) *ACSM/ASPRS Ann. Conv. 3*, 256; — (1995) *Z. Phot. Fern. 63*(1) 4. [15] Reid, M. (2009) *SIS For Mini-RF Advanced Technologies Lunar Reconnaissance Orbiter (LRO) Payload Operations Center*, Document MRF-4009. [16] Batson, R.M. (1990) in *Planetary Cartography*, 60–95. [17] Acton, C.H. (1999) *LPS XXX*, 1233. [18] Beyer, R. et al. (2010) *LPS XLI*, this conference. [19] Kirk, R.L. et al. (2009) *LPS XL*, 1414.

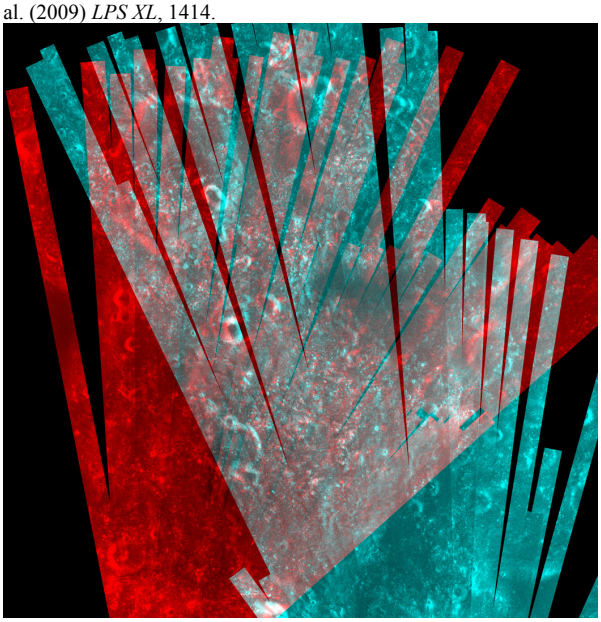

Figure 1. Anaglyph formed by combining uncontrolled mosaics of left- and right-looking LRO Mini-RF S-zoom mode images, to be viewed with red lens on the left eye and blue-green on the right. Polar Stereographic projection with south approximately at the bottom. The 98-km crater Cabeus occupies the bottom portion of the area of overlapping coverage. Cabeus B is to the upper left and Cabeus A at top center.